

Array Pattern Synthesis of Multiband Hexagonal Fractal Antenna Array for Reduced Sidelobe and Deep Null Control using Modified Invasive Weed Optimization Algorithm

Krishna Kanth Varma P¹, Nagesh K N²

¹Asst Professor, ECE Department, SRKR Engineering College, Bhimavaram, AP, India,
varmakk.pen2@gmail.com

²Professor, ECE Department, Nagarjuna College of Engineering and Technology, Bangaluru, Karnataka, India
kn.nagesh@nacetmail.com

ABSTRACT

Design of antenna arrays involving fractal concepts have resulted in the evolution of new fractal antenna array geometries that exhibit multiband characteristics. In this paper array pattern synthesis of hexagonal fractal antenna array (HFAA) is proposed for imposing symmetric nulls in the interference directions while maintaining a reduced side lobe level (SLL) using a modified invasive weed optimization algorithm (MIWO). The desired characteristics are obtained by optimizing the current amplitude coefficients of HFAA. Further multiband characteristics of the fractal array are investigated. The results indicate the improved performance of MIWO when compared to conventional invasive weed optimization algorithm (IWO) in achieving the desired radiation characteristics. Also optimized HFAA demonstrates multiband behavior in achieving similar radiation characteristics.

Key words: Pattern nulling, fractal arrays, multiband arrays, invasive weed optimization, sidelobe level.

1. INTRODUCTION

The evolution of 5G communication systems has provided new challenges in the antenna design methodology in the sub 6GHz band and mmWave frequency band [1]. The requirement to produce optimized radiation characteristics has led to a significant interest in the design of large scale antenna arrays that can operate at multiple frequencies. On the other hand the increase in 5G applications will lead to increase in interfering signals. The need to design antenna arrays with reduced SLL and imposed deep nulls in the interfering directions has become vital [2]. Array pattern synthesis problem of imposing nulls and reducing SLL for conventional antenna array geometries have been explored using novel global optimization techniques. Some studies have concentrated on reducing Side Lobe Level (SLL) of linear and planar arrays for a constant beam width utilizing evolutionary

optimizing techniques such as Differential Evolution (DE) and Moth Flame Optimization (MFO) [3],[4]. Other studies have worked on array pattern synthesis aimed at producing prescribed nulls in the interference direction so as to suppress the unwanted interference. A modified differential evolution algorithm is proposed for introducing asymmetric nulls of 28 element linear antenna array [5]. In [6] investigation into pattern nulling of uniform linear array and non-uniform circular array has been carried out by applying novel IWO/DWO algorithm. Positioning of single nulls as well as broad nulls in the interference direction was explored and compared with various benchmark functions. A nature inspired technique of firefly algorithm applied for optimizing amplitude coefficients to produce minimum SLL with nulls, yielded a null depth of -80dB [7]. IWO as a metaheuristic algorithm was effectively applied for control of SLL as well as desired nulls for a planar array [8]. Over the years few variations of IWO have been explored to a great degree of success in tackling null control problem of conventional antenna arrays [9], [10].

The ability of an antenna to radiate at multiple frequencies has led to its rampant utilization in the fields of 5G, satellite, RADAR and other wireless communications. A renowned approach followed in the design of multiband antennas has been the application of Fractal theory concepts. The self-similar and repetitive geometrics properties of fractal shapes such as Koch curve, peano curve and other shapes have aided in achieving both multiband and UWB characteristics of portable microstrip antennas[11][12][13][14]. The self-scaling properties of fractals are also applied in the construction of fractal arrays. A fractal array can be constructed by repetitively applying a conventional array known as generating subarray at different regular scales, positions and directions [15]. A common subarray generator used is concentric ring antenna array. Several planar fractal arrays can be generated using concentric subarray generator. Apart from having high directivity fractal arrays offer distinct advantage over conventional arrays in the form multiband operation with respect to radiation characteristics [16]. The main drawback of uniform fractal arrays has been the relatively high SLL and the increase of large number of

elements at higher growth stages. A new design methodology was recently presented for SLL reduction of thinned Hexagonal and pentagonal fractal arrays using Ant Colony optimization [17]. Further least mean square algorithm was also applied for Adaptive beam forming strategy.

The present paper is aimed at addressing the constraints Hexagonal Fractal Antenna Array (HFAA) by using modified invasive optimization algorithm (MIWO). The objectives include Imposing deep nulls in the prescribed directions, reducing the SLL, Exploring the multiband characteristics of HFAA, comparison of MIWO and IWO.

2. DESIGN OF HEXAGONAL FRACTAL ANTENNA ARRAY (HFAA)

A fractal antenna array can be generated by repetitive application of a generating subarray. The generating subarray is copied and scaled with a certain scaling factor $P > 1$. Additionally the elements of the subarray are selectively turned on and off to generate the required fractal array [13]. One common generating subarray used is the concentric circular antenna array (CCAA). The array factor of CCAA with M concentric rings and each ring having N_m elements is expressed as [18].

$$GA(\theta, \phi) = \sum_{m=1}^M \sum_{n=1}^{N_m} I_{mn} e^{j\varphi_{mn}(\theta, \phi)} \tag{1}$$

Where

$$\varphi(\theta, \phi) = kr_m \sin\theta \cos(\phi - \phi_{mn}) + \alpha_{mn} \tag{2}$$

Where I_{mn} and α_{mn} denote the amplitude and phase excitations of n^{th} element in the m^{th} ring. $K=2\pi/\lambda$ is the phase constant and λ is the wavelength. Θ and ϕ denote the elevation and azimuth angle.

With CCAA in (1) as the generating subarray, the array factor of HFAA is expressed as

$$AF(\theta, \phi) = \prod_{p=1}^P \sum_{m=1}^M \sum_{n=1}^{N_m} I_{pn} e^{j\delta^{p-1}\varphi_{pn}(\theta, \phi)} \tag{3}$$

Where δ is the expansion ratio and P is the number of growth stages. For an HFAA the CCAA of 6 element ring is used as the subarray generator. The elements of the subarray are positioned on the perimeter of the concentric rings to attain the desired fractal geometry. For a self-scalable HFAA to generate the expansion ratio is observed to be 2. Thus the AF in (3) for a radius of $\lambda/2$ is modified to [17]

$$AF(\theta, \phi) = 1/6^P \prod_{p=1}^P \sum_{n=1}^6 I_{pn} e^{j2^{p-1}\varphi_{pn}(\theta, \phi)} \tag{4}$$

Where

$$\varphi_n(\theta, \phi) = \Pi \sin\theta \cos(\phi - \phi_n) + \alpha_n \tag{5}$$

$$\phi_n = \Pi/3 (n-1) \tag{6}$$

$$\alpha_n = \Pi \sin\theta \cos(\phi - \phi_n) \tag{7}$$

ϕ_0 and θ_0 represent the steering angles.

The geometry of HFAA for three growth stages is shown in Figure 1.

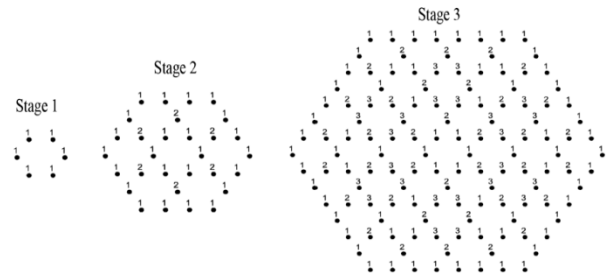


Figure 1. Geometrical representation of First three stages of HFAA

3. INVASIVE WEED OPTIMIZATION ALGORITHM (IWO)

IWO is a meta-heuristic algorithm that mimics the colonizing behavior of weeds. It was first introduced by Mehrabian and Lucas in 2006 [19]. The seeds are dispersed randomly over the fields by invading weeds. These seeds develop into weeds utilizing the random spaces. Those adequately adapted weeds (good fitness) produce higher number of seeds than lowly adapted weeds. These new weeds are dispersed in the field further with a standard deviation and they grow into flowering weeds and the process continues. This competition among the weeds results in a colonizing behavior. The algorithm can be explained in a four step process.

- I) Initialization: A fixed number of initial seeds are generated and distributed randomly in prescribed limits.
- II) Reproduction: The fitness of each seed is first evaluated. The seeds are now referred as flowering weeds. Each weed is allowed to generate new seeds based on the fitness. The maximum and minimum number of seeds generated is limited between values S_{max} and S_{min} .
- III) Spatial Distribution: Two different variations are explored in this step.

Conventional IWO (IWO): The newly generated seeds are dispersed using a standard deviation function given as.

$$\sigma_{iter} = \frac{(iter_{max} - iter)^n}{(iter_{max})^n} (\sigma_{ini} - \sigma_{fin}) + \sigma_{fin} \tag{8}$$

Where σ_{ini} and σ_{fin} denote the initial and final standard deviation values, respectively.

Modified IWO (MIWO): To verify if the conventional IWO is sensitive to initialization and to overcome the problem of trapped local optima solution, a variation in spatial distribution is tested. Here half of the generated seeds with better fitness function are dispersed using the function (8). The other half of the generated seeds with lower fitness function are dispersed using the below equation.

$$S_{new} = rand * S_{best} + rand * S_{worst} \tag{9}$$

Where S_{new} is the newly generated seed, S_{best} and S_{worst} are weeds with best fitness and worst fitness for each iteration.

IV) Competitive exclusion: Inorder to control the population explosion of the newly generated seeds for every passing iteration the seeds with better fitness are limited to a maximum number of weeds P_{max} . The above steps I to IV are repeated until the termination criteria is met.

4. PROBLEM FORMULATION

In order to optimization the radiation pattern for the desired objective, the fitness function is formulated as below [20].

$$FF = w_1 \frac{|\prod_{i=1}^m AF(null_i)|}{|AF_{max}|} + w_2 (SLL_{cur} - SLL_{des}) + w_3 |HPBW_{cur} - HPBW_{des}| \quad (10)$$

In the first term $AF(null_i)$ denotes the array factor at the null position, whereas AF_{max} represents the maximum value of array factor. This term controls the positions of the nulls. In the second term SLL_{cur} represents the SLL for the current iteration and SLL_{des} represents the desired SLL. In the third term $FNBW_{cur}$ represents the first null beam width of the main lobe for the current iteration and $FNBW_{des}$ represents the desired first null beam width. w_1, w_2, w_3 represent the weighting coefficients to control nulls, SLL, FNBW respectively.

The IWO algorithm is applied with the following control parameters in Table 1.

Table 1. Control parameters for IWO algorithm

| Control parameter | Value |
|---|----------|
| Initial no of seeds | 10 |
| Maximum no of seeds S_{max} | 5 |
| Minimum no of seeds S_{min} | 1 |
| Maximum no of flowering weeds | 10 |
| Initial Standard deviation σ_{ini} | 0.05 |
| Final Standard deviation σ_{fin} | 0.000001 |
| Modulation index n | 3 |

5. RESULTS and DISCUSSION

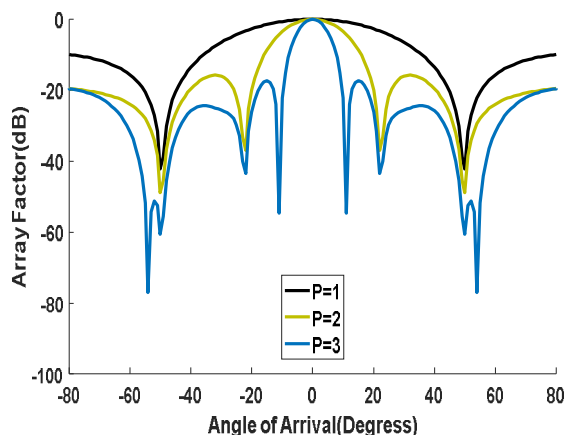


Figure 2. Array Factor of HFAA for different growth stages.

The uniform HFAA radiation pattern for the growth stages of P 1,2,3 for $r=\lambda/2$ are shown in Figure 2.

Table 2. Radiation Characteristics of HFAA for different growth stages.

| Growth stage (P) | Number of elements | SLL(dB) | HPBW($^\circ$) |
|------------------|--------------------|---------|------------------|
| 1 | 6 | -10 | 51 |
| 2 | 30 | -15.84 | 23 |
| 3 | 132 | -17.31 | 11 |

As is evident from table 2 HFAA has improved HPBW for increase in each growth stage but with a relatively high SLL. IWO algorithm is applied to simultaneously reduce the SLL of HFAA at P=3 and impose symmetric nulls in the prescribed directions. The algorithm is applied to optimize the amplitude coefficients of HFAA using MATLAB software. Fig 3 shows the array factor of optimized HFAA using IWO and MIWO for imposed symmetric nulls in three random directions 60° , 77° , 51° . Table 3 lists the Comparison of the optimized parameters using the two algorithms.

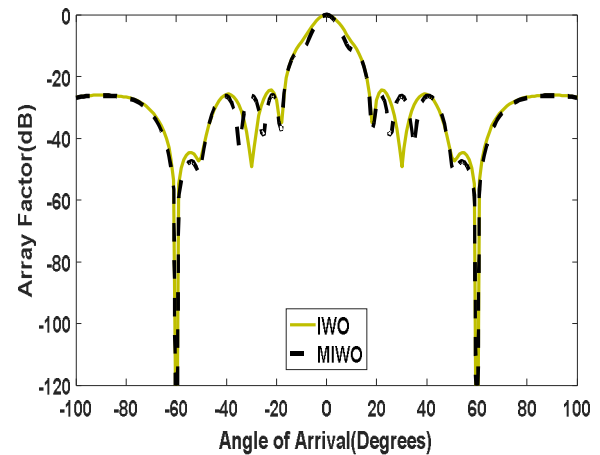


Figure 3a. Array factor of optimized HFAA for P=3, $r=0.5 \lambda$ with nulls at $[-60^\circ 60^\circ]$

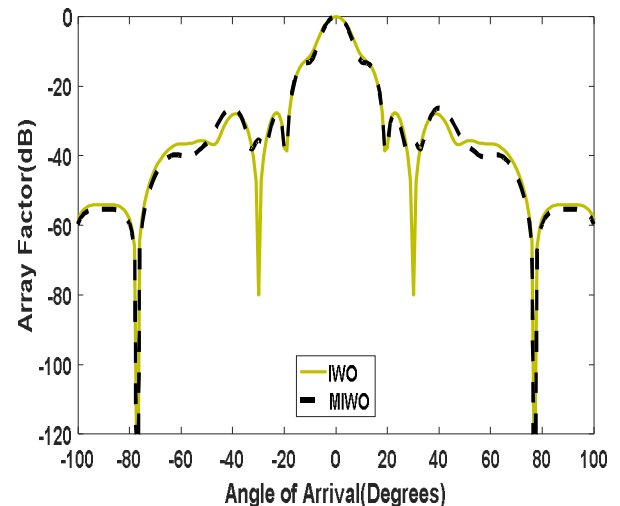


Figure 3b. Array factor of optimized HFAA for P=3, $r=0.5 \lambda$ with nulls at $[-77^\circ 77^\circ]$

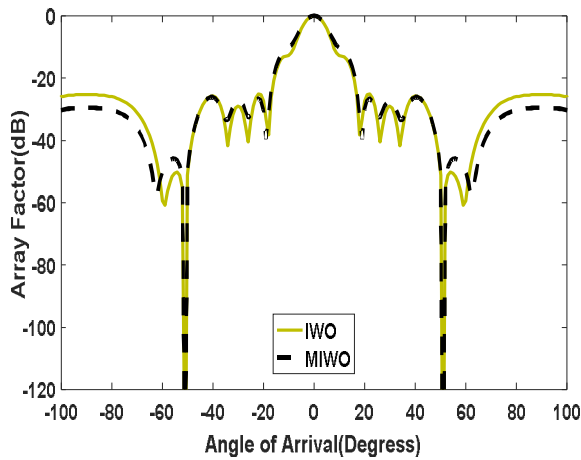


Figure 3c. Array factor of optimized HFAA for P=3, r=0.5 λ with nulls at [-51° 51°]

Table 3. Comparison of Optimized SLL and Null depth at the prescribed directions for HFAA with r=0.5 λ between IWO, MIWO.

| | Null Directions (°) | -60° & 60° | -77° & 77° | -51° & 51° |
|------|---------------------|------------|-----------------|------------|
| | | IWO | Null Depth (dB) | -166.6 |
| | SLL (dB) | -24.37 | -27.63 | -25.18 |
| | HPBW (°) | 18 | 19 | 18 |
| MIWO | Null Depth (dB) | -169.2 | -166 | -164.9 |
| | SLL (dB) | -26.02 | -28.23 | -26.55 |
| | HPBW (°) | 18° | 19° | 18° |

In case I for imposing nulls along -60° & 60° the IWO optimized HFAA yielded a SLL of -24.37dB with null depth of -166.6dB and HPBW of 18°, while MIWO optimized HFAA yielded a SLL of -26.02dB with null depth of -169.2dB and HPBW of 18°. In case II for imposing nulls along -77° & 77° the IWO optimized HFAA yielded a SLL of -27.63dB with null depth of -148.9dB and HPBW of 19°, while MIWO optimized HFAA yielded a SLL of -28.23dB with null depth of -166dB and HPBW of 19°. In case III for imposing nulls along -51° & 51° the IWO optimized HFAA yielded a SLL of -25.18dB with null depth of -167.9dB and HPBW of 18°, while MIWO optimized HFAA yielded a SLL of -26.55dB with null depth of -164.9dB and HPBW of 18°. The results indicate a better performance of MIWO in reducing the SLL for all the three cases and imposing the better null depth in two of the cases (I & II) when compared to conventional IWO. The fractal arrays are known to exhibit multiband characteristics by maintaining similar radiation pattern for a different wavelength determined by the expansion ratio δ_n from the initial wavelength of $r=0.5\lambda$, where n ranges from 1 to P-1 [6]. For HFAA, $\delta=2$ and with

$P=3, n=1,2$ which results in a possible second operating wavelength of $r=0.25\lambda$. The multiband band characteristics of optimized HFAA are practically investigated for a radius $r=0.25\lambda$, results shown in figure 4 with comparison of optimized parameters listed in Table 4.

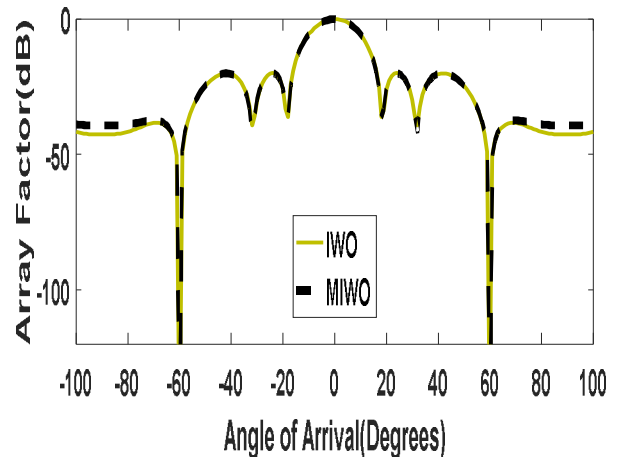


Figure 4a. Array factor of optimized HFAA for P=3, r=0.25 λ with nulls at [-60° 60°]

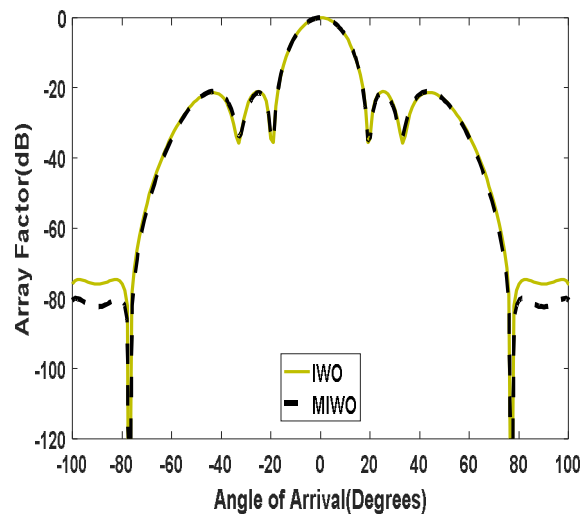


Figure 4b. Array factor of optimized HFAA for P=3, r=0.25 λ with nulls at [-77° 77°]

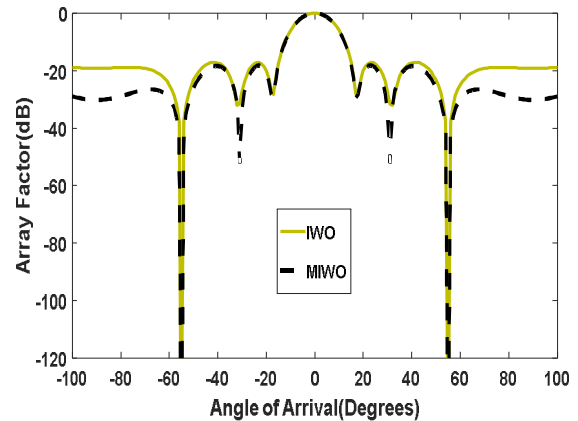


Figure 4c. Array factor of optimized HFAA for P=3, r=0.25 λ with nulls at [-55° 55°]

Table 4. Comparison of Optimized SLL and Null depth at the prescribed directions for HFAA with $r=0.25 \lambda$ between IWO,MIWO.

| | Null Directions (\square) | -60 & 60 | -77 & 77 | -55 & 55 |
|------|-------------------------------|--------------|--------------|--------------|
| IWO | Null Depth (dB) | -147.1 | -161.2 | -147.1 |
| | SLL (dB) | -20.25 | -21.04 | -17.18 |
| | HPBW (\square) | 18 | 19 | 17 |
| MIWO | Null Depth (dB) | -162.2 | -164.9 | -162.4 |
| | SLL (dB) | -20.24 | -21.64 | -18.49 |
| | HPBW (\square) | 18 \square | 19 \square | 17 \square |

In case I for imposing nulls along -60° & 60° the IWO optimized HFAA yielded a SLL of -20.25dB with null depth of -147.1dB and HPBW of 18° , while MIWO optimized HFAA yielded a SLL of -20.24dB with null depth of -162.2dB and HPBW of 18° . In case II for imposing nulls along -77° & 77° the IWO optimized HFAA yielded a SLL of -21.04dB with null depth of -161.2dB and HPBW of 19° , while MIWO optimized HFAA yielded a SLL of -21.64dB with null depth of -164.9dB and HPBW of 19° . In case III for imposing nulls along -51° & 51° the IWO optimized HFAA yielded a SLL of -17.18dB with null depth of -147.1dB and HPBW of 17° , while MIWO optimized HFAA yielded a SLL of -18.49dB with null depth of -162.4dB and HPBW of 17° . The results indicate the better performance of MIWO over IWO in imposing a deeper null depth for all the three cases, while providing a better reduced SLL for case III. Also evident from the results is the ability of optimized HFAA in imposing nulls with reduced SLL and fixed HPBW less than 20° at multiple frequencies corresponding to $r=0.5 \lambda$ and $r=0.25 \lambda$. Figure 5 shows the comparison between MIWO optimized HFAA for $r=0.5 \lambda, 0.25 \lambda$ with a similar 132 element MIWO optimized CCAA for $r=0.5 \lambda, 0.25 \lambda$. For $r=0.5 \lambda$ optimization of CCAA resulted in a similar reduction of SLL and null depth but with larger HPBW of 22° , whereas for $r=0.25 \lambda$ the optimization of CCAA failed in imposing the nulls and also with an increased HPBW of 40° . Figure 6 shows the comparison of convergence performance of MIWO and IWO for a test case when optimizing HFAA for imposed nulls in $-60^\circ, 60^\circ$. Comparison shows better performance of MIWO in both convergence rate and value over IWO for both wavelengths of the array.

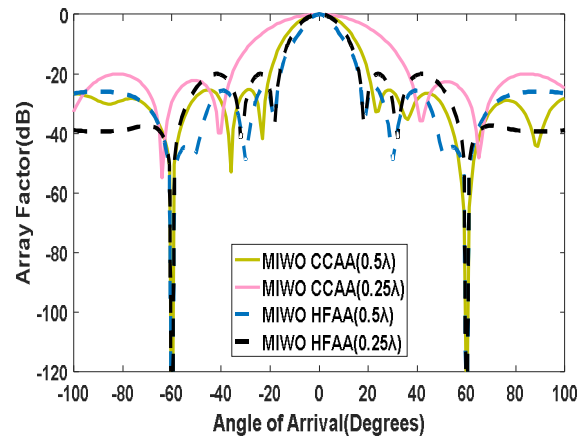


Figure 5. Array factor of optimized CCAA and HFAA for $P=3, r=0.5 \lambda, 0.25 \lambda$ with nulls at $[-60^\circ, 60^\circ]$

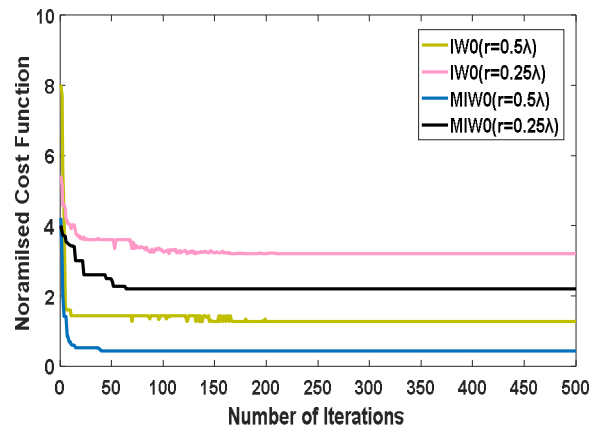


Figure 6. Comparison of convergence of cost functions vs. number of iterations between IWO and MIWO.

Table 5 shows a sample set of current amplitude coefficients of optimized HFAA for $r=0.5 \lambda$.

| Radius | Null Directions | Amplitude coefficients $I_{pn}, p=1, \dots, P$ & $n=1, \dots, N$ |
|-------------------------|-----------------------------|--|
| 0.5 λ | $[-60^\circ, 60^\circ]$ | 0.2482 0.6871 0.7835 0.8303 0.1725 0.4212 |
| | | 0.9294 0.3963 0.3563 0.9602 0.3613 0.2651 |
| | | 0.5617 0.0076 0.7765 0.9470 0.2171 0.1160 |
| | $[-77^\circ, 77^\circ]$ | 0.5743 0.1945 0.1157 0.3755 0.3620 0.3665 |
| | | 0.6069 0.5705 0.4271 0.5928 0.1529 0.0376 |
| | | 0.5171 0.4116 0.4753 0.9451 0.6987 0.0290 |
| $[-51^\circ, 51^\circ]$ | 0.3126 0.5265 0.5631 0.7127 | |

| | | |
|----------------|-------------|--|
| | | 0.4429 0.7539 0.5501 0.1611 0.0174 0.6002 0.5189 0.3620 0.3166 0.0596 0.5044 0.9493 0.2976 0.0574 |
| 0.25 λ | [-60°, 60°] | 0.8466 0.0113 0.0023 0.8589 0.0012 0.0025 0.8180 0.1280 0.0166 0.9186 0.0227 0.0421 0.9569 0.6068 0.4188 0.9428 0.2616 0.0992 |
| | | 0.8057 0.0531 0.0046 0.8413 0.0125 0.1678 0.8077 0.2280 0.0178 0.8974 0.1067 0.0713 0.7492 0.5420 0.3565 0.6758 0.4172 0.1330 |
| | | 0.9648 0.1038 0.0720 0.9271 0.0736 0.0216 0.9802 0.0060 0.0301 0.9614 0.0766 0.0766 0.9584 0.3136 0.1933 0.9607 0.2988 0.1513 |

5. CONCLUSION

In this paper pattern synthesis of HFAA is proposed to achieve desired radiation characteristics at multiple frequencies. A MIWO algorithm is applied to optimize the current amplitude coefficients of HFAA to impose nulls in the required directions while maintaining a reduced SLL. The performance of the MIWO is compared with IWO. The results show an improved performance of MIWO in imposing deeper nulls with a reduced SLL and also in rate of convergence. This work also demonstrates the superiority of optimized HFAA when compared to its subarray generator CCAA in producing similar radiation pattern at multiple frequencies.

REFERENCES

1. T.S. Rappaport, S. Sun, R. Mayzus, H. Zhao, Y. Azar, K. Wang, G.N. Wong, J.K. Schulz, M. Samimi and F. Gutierrez, **Millimeter Wave Mobile Communications for 5G Cellular: It Will Work!**, *IEEE Access*, vol. 1, pp. 335-349, May 2013.
2. J.R. Mohammed and K.H. Sayidmarie, **Sidelobe Nulling**

by **Optimizing Selected Elements in the Linear and Planar Arrays, in Array Pattern Optimization**, *IntechOpen*, pp. 1-24, 2019.

3. A. Deb, J.S. Roy and B. Gupta, **Differential Evolution Algorithms Perform in Designing Microstrip Antennas and Arrays**, *IEEE Antennas and Propagation Magazine*, vol. 60, no. 1, pp. 1-11, Feb. 2018.
4. A. Das, D. Mandal, S.P. Ghoshal and R. Kar, **Concentric circular antenna array synthesis for side lobe suppression using moth flame optimization**, *Int. J. Electron. Commun. (AEÜ)*, vol. 86, pp. 177-184, March. 2018.
5. S.V.R. Rao, A.M. Prasad and Ch, S. Rani, **Antenna Array Pattern Nulling by Phase Perturbations using Modified Differential Evolution Algorithm**, *International Journal of Emerging Trends in Engineering Research*, vol. 7, no. 9, pp. 256-261, September 2019.
6. S.K. Mahto and A. Choube, **A novel hybrid IWO/WDO algorithm for nulling pattern synthesis of uniformly spaced linear and non-uniform circular array antenna**, *International Journal of Electronics and Communications (AEÜ)*, vol. 70, pp. 750-756, 2016.
7. S. Mubeen, A.M. Prasad and A.J. Rani, **Amplitude-Only Null Positioning in Linear Arrays Using Firefly Algorithm**, in *proc, in IEEE WiSPNET 2017 conference*, Chennai, 2017.
8. H.N. Wu and C. Liu, **Planar array synthesis with sidelobe reduction and null control using invasive weed Optimization**, *Progress in Electromagnetic Research M*, vol. 33, pp. 83-94, 2013.
9. G.G. Roy, S. Das, P. Chakraborty and P.N. Suganthan, **Design of Non-Uniform Circular Antenna Arrays Using a Modified Invasive Weed Optimization Algorithm**, *IEEE Trans. Antennas Propag*, vol. 59, no. 1, pp. 110-118, 2011.
10. E.H. Kenane, F. Djahli and C. Dumond, **A Novel Modified Invasive Weeds Optimization for Linear Array Antennas Null Control**, in *4th International Conference on Electrical Engineering*, Boumerdes, 2015.
11. V.V. Reddy and N.V.S.N. Sarma, **Triband Circularly Polarized Koch Fractal Boundary Microstrip Antenna**, *IEEE Antennas and Wireless Propagation Letters*, vol. 13, pp. 1057-1060, May. 2014.
12. P. Krishna Kanth Varma, Ch. Murali Krishna and Dr.P.V.Rama Raju, **A Multiband Slotted Log Periodic Dipole Array Antenna Design using Giuseppe Peano Fractal Geometry**, in *IEEE 2018 4th International Conference on Applied and Theoretical Computing and Communication Technology (iCATccT)*, 2018.
13. W.C. Weng and C.L. Hung, **An H-Fractal Antenna for Multiband Applications**, *IEEE Antennas and Wireless Propagation Letters*, vol. 13, pp. 1705-1708, Aug. 2014.
14. P.K.K. Varma and B. Sitaram, **Design of Ultra Wide Band Trapezoidal Antenna for Wireless and Satellite**

Applications, *International Journal of Emerging Trends in Engineering Research*, vol. 8, no. 9, pp. 6210-6213, September 2020.

15. D.H. Werner, R.L. Haupt and P.L. Werner, **Fractal Antenna Engineering: The Theory and Design of Fractal Antenna Arrays**, *IEEE Antennas and Propagation Magazine*, vol. 41, no. 5, pp. 37-59, Oct. 1999.
16. Hussein, R.A.T, Jibrael Jabri and F.J., **Comparison of the Radiation Pattern of Fractal and Conventional Linear Array Antenna**, *Prog, Electromagn. Res*, vol. 4, p. 183–190, 2008.
17. S.E. EL-Khamy, A.S. Eltrass and H.F. El-Sayed, **Design of Thinned Fractal Antenna Arrays for Adaptive Beam Forming and Sidelobe Reduction**, *IET Microw. Antennas Propag.*, vol. 12, no. 3, pp. 435-441, Jan. 2018.
18. D. Mandal and A. Chandra, **Side Lobe Reduction of a Concentric Circular Antenna Array using Genetic Algorithm**, *Serbian Journal of electrical engineering*, vol. 7, no. 2, pp. 141-148, Nov. 2010.
19. A.R. Mehrabian and C. Lucas, **A novel numerical optimization algorithm inspired from weed colonization**, *cological Informatics*, vol. 1, no. 4, pp. 355-366, Dec. 2006.
20. T.R.S. Raj, P.K.K. Varma and P.V.R. Raju, **Invasive Weed Optimization (IWO) Algorithm for Control of Nulls and Sidelobes in a Conectric Circular Antenna Array (CCAA)**, *International Journal of Computer Applications*, vol. 126, no. 3, pp. 44-49, 44-49.